

Ultra-broadband active noise cancellation at the ears via optical microphones

Tong Xiao¹, Xiaojun Qiu¹ & Benjamin Halkon¹

¹Centre for Audio, Acoustics and Vibration (CAAV), University of Technology Sydney, Sydney, NSW 2007 Australia. Correspondence and requests for materials should be addressed to T.X. (Tong.Xiao@student.uts.edu.au) or to X.Q. (Xiaojun.Qiu@uts.edu.au)

Abstract

High frequency noise has generally been difficult to be cancelled actively at a person's ears, particularly for active headrest systems aiming to free the listener from noise cancellation headphones. One of the main challenges is to measure the noise precisely at the ears. Here we demonstrate a new error sensing methodology with an optical microphone arrangement for active noise cancellation (ANC). It can measure the noise accurately for ANC without any obstructions at the listener's ears. The demonstrated system, or virtual ANC headphone as we call it, is shown to provide more than 10 dB attenuation for ultra-broadband noise – up to 6000 Hz – inside the ears in a complex sound field. The bandwidth of the controllable noise significantly exceeds the results from the state-of-the-art system, which is below 1000 Hz. The proposed method leads to the next generation of personal hearing protection system and can open up a whole new area of sound control research.

Introduction

Long-term exposure to either occupational or environmental noise can lead to a series of diseases, both auditory¹ and non-auditory^{2,3}. Global active noise cancellation (ANC) reduces noise in a large environment, but requires a large number of control loudspeakers, making it impractical for many applications⁴. By contrast, local ANC aims to reduce noise at specific local positions, which are often around a listener's ears. One of the most popular applications is ANC headphones. The cushion and shell structure of earmuffs provide *passive* sound attenuation in the middle to high frequency range for hearing protection^{5,6}. The *active* sound control part, on the other hand, generates a secondary “anti-noise” with the same amplitude but an opposite phase of the primary noise via the speakers inside, to provide good noise reduction in the low frequency range^{7,8}. ANC headphones are commonly used in aircrafts, where noise from the aircraft during long haul flights is known to be detrimental on health^{3,9}. However, long-term wear of these headphones can cause discomfort and/or fatigue¹⁰. Devices that can provide noise reduction in the ears like earmuffs and ANC headphones, but without having to wear anything (i.e., the “virtual ANC headphones” proposed in this paper), are desired in many scenarios such as for drivers in vehicles^{11,12} and for people working in open offices¹³.

A substantial amount of effort has been made to move the loudspeakers and sensors of ANC systems away from a person's ears^{14–19}. For example, in an active headrest system, both secondary loudspeakers and error microphones are installed at the back of a person's seat to cancel the noise at the two ears¹⁴. Due to the difference between the sound pressure measured at the error microphones (which, due to their size, cannot be placed directly in the ears where the pressure needs to be measured) and that at the listener's ears, cancelling noise at the remote error microphone locations cannot guarantee good noise reduction at listener's ears, particularly in the higher frequency range where wavelength of sound is small. Many virtual sensing algorithms have been proposed to estimate the sound pressure at the ears based on the signals obtained from the physical microphones positioned at alternative locations, somewhat remote from the ears^{20–25}. However, even with many microphones and complicated algorithms, the upper limit frequency for effective noise cancellation in the ears is still relatively low.

For example, using an array of four microphones and a head tracking system (to determine the position of the head and therefore optimise the error signal estimation algorithm even in the presence of head movement), an active headrest system recently developed (the state of the art) can only achieve good noise reduction up to 1000 Hz for noise coming from one specific direction^{25,26}.

Acoustic metamaterials, which are artificially engineered materials without the usual characteristic limitations of their natural equivalents, have been developed recently to prevent the propagation of acoustic waves^{27,28}. Advances in both passive^{29–31} and active^{32–35} acoustic metamaterial technologies demonstrate their impressive control ability on the noise, which can be either absorbed or redirected. Specifically, the non-reciprocal and nonlinear active acoustic metamaterials allow only one-way propagation^{32,33}, which can isolate the noise from the listener. However, it is hard for these new materials to generate a quiet zone in a complicated sound field at present.

Acousto-optical technology, which uses light to obtain acoustical information, was first proposed more than 100 years ago³⁶. An interferometer can be employed to sense the displacement of a membrane due to changes in pressure. Similarly, a laser Doppler vibrometer (LDV)³⁷ makes use of interferometric optical arrangements to detect the Doppler frequency shift of a vibrating body, resulting in surface velocity measurements. Due to its high sensitivity and non-intrusiveness, this device is used in a wide range of scenarios including medical diagnostics^{38–40} and mechanical system evaluation^{41–43}. By using an LDV with a small size membrane that responds well to sound pressure fluctuations, an optical microphone arrangement can be constructed to obtain an error signal, alternative to that of the conventional microphone, for noise cancellation purposes.

In this research, we report a new error sensing methodology to reduce the noise at the user's ears for personal hearing protection. Our proposed active noise cancellation system is more suitable for personal hearing protection than any known metamaterial equivalent solutions presented thus far and can reduce noise in a person's ears over an extended frequency range up to 6000 Hz. Because our system does not have any actuators, sensors or materials around the ears, it is named as a "virtual ANC headphone". The so-called virtual ANC headphone is a natural extension of current ANC headrest systems, but neither

installs any error microphones on or near the listener's head, nor uses any kind of virtual sensing methodologies to estimate the sound pressure at the ears. The proposed system obtains the noise propagating into the ear canals directly by using an acousto-optical transducer combination, which is formed from an LDV and a lightweight membrane corresponding to sound pressure fluctuations. The experimental results are reported herein to illustrate its performance.

Results

Virtual active noise cancellation (ANC) headphones design. The schematic of the proposed system is shown in Fig. 1a. An LDV is used to obtain the sound in each ear by measuring the vibration of the membrane (caused by the sound) located therein. Two loudspeakers are placed behind the head (e.g., on a headrest) at two sides to cancel the primary noise in each ear. A quiet zone is accomplished around the membrane with a diameter of a tenth of the primary noise wavelength with a benchmark 10 dB reduction⁴⁴. When the membrane is placed in the ear, this quiet zone can extend over the ear canal, reducing the noise propagating to the tympanic membrane. The head movements are tracked by a camera-based tracking system, which actively controls a pair of orthogonal, galvanometer-driven mirrors which steer the probe laser beam to the centre of the membrane. Thus, the LDV measures the error signals for the ANC system in real-time accurately via a special image processing algorithm (details in the Methods section).

The locations of the secondary loudspeakers, which are used to generate the anti-noise signal to cancel the noise, are flexible. As an example, Fig. 1b shows that the listener is at the central location and each secondary loudspeaker is placed 0.24 m away from the centre of the listener's head. The two loudspeakers are 0.44 m apart with an azimuth angle of 45 degrees pointing to the listener. The anti-noise signals for the secondary loudspeakers are calculated by the ANC controllers at each side separately. Each controller takes the primary noise signal as the reference signal and the vibration velocity of the membrane from an LDV as the error signal (details in the Methods section).

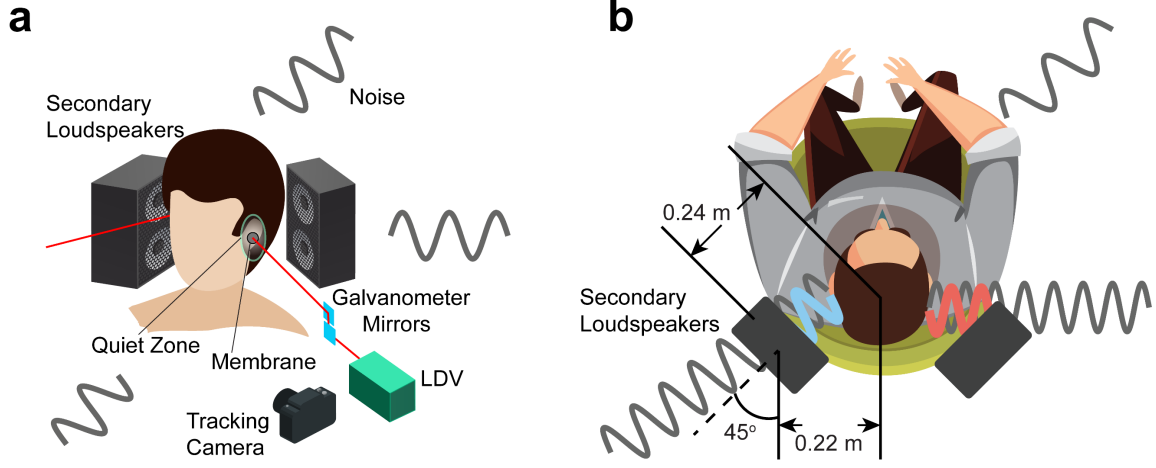


Figure 1. A virtual active noise cancellation (ANC) headphone. **(a)** A quiet zone is formed in each ear when using a secondary loudspeaker nearby to cancel the noise. The error signal is from the optical microphone, which is made up from the laser Doppler vibrometer (LDV) and a membrane located in the ear. The movement of the listener is tracked by a camera-based tracking system, which actively controls the galvanometer-driven mirrors to steer the laser beam and maintain its position on the membrane when the user's head moves. **(b)** The secondary loudspeakers are placed 0.24 m away from the centre of the listener's head with a tilting angle of 45 degrees and are 0.44 m away from each other. Each secondary loudspeaker generates anti-noise signals for each ear through the ANC controllers.

A circular membrane is used with the LDV to measure the residual sound in the ear. The mathematical expression of the motion of a circular membrane in the cylindrical coordinates can be written as^{45,46}

$$\nabla^2 \eta(r, \theta) + K^2 \eta(r, \theta) = -\frac{p_i}{T} + \frac{p(r, \theta, 0)}{T}, \quad 0 < r < a \quad (1)$$

where $\eta(r, \theta)$ is the vertical membrane displacement, p_i is the incident sound pressure, $p(r, \theta, 0)$ is the reaction pressure at the membrane surface and a is the radius of the membrane. K is the wave number of the membrane, with $K = \omega \sqrt{\sigma_M / T}$, where ω is the angular frequency, σ_M is the membrane mass

surface density and T is the tension of the membrane. By applying the Dirichlet boundary conditions^{46,47} $\eta(r = a, \theta) = 0$, a zeroth-order approximation of the membrane velocity can be expressed as

$$v_z(r, \theta, 0) = \frac{j\omega}{K^2 T} p_i \left[\frac{J_0(Kr)}{J_0(Ka)} - 1 \right] \quad (2)$$

where j is the complex number, J_0 is the zero order Bessel function of the first kind. It represents an approximation of the membrane velocity with respect to the incident sound pressure. Therefore, the sound pressure can be determined by measuring the vibration velocity of the membrane.

Figure 2a shows the experimental setup. The experiment is performed in a quiet laboratory with a background noise of 38.5 dBA. In the stationary test (the head is not moving), a head and torso simulator (HATS) is used, where the output signals from the ear simulators are used to represent the sound at the tympanic membranes in ears approximately. At each side, the error signal from the optical microphone goes to the ANC controller for generating the control sound adaptively to cancel the primary noise.

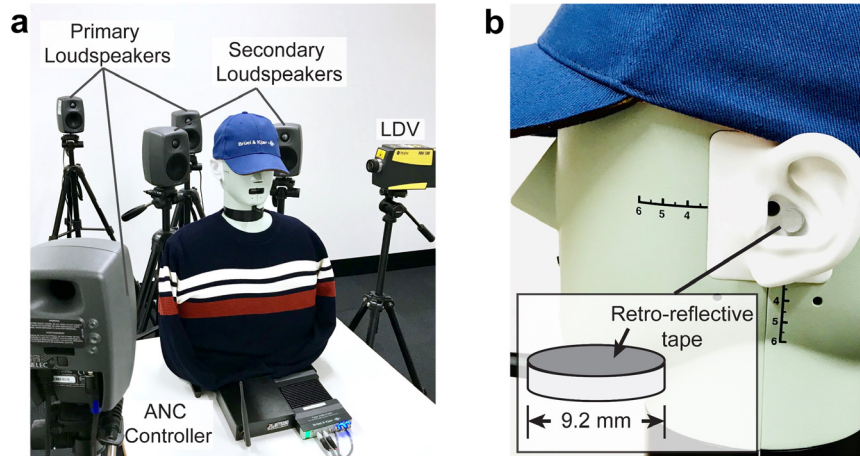


Figure 2. Experimental setup for a stationary subject. **(a)** Two secondary loudspeakers are placed behind the head for noise cancellation. Multiple primary loudspeakers (three shown here for clarity) are located randomly around to simulate the unwanted noise from different directions simultaneously. A laser Doppler vibrometer (LDV) is directed towards the membrane in the ear. **(b)** A membrane placed in an ear (only the left one is shown here) of a head and torso simulator (HATS).

The membrane used in this system is shown in Fig. 2b. It is comprised of a piece of retro-reflective tape bound to a circular substrate with a diameter of 9.2 mm. It is produced to be as minimally non-invasive as practically possible. The retro-reflective tape is used to maximise the backscattered optical signal in relation to the inbound laser beam, irrespective of a non-normal beam incidence. The membrane needs to be flexible enough to vibrate by responding to the noise across the frequency range of interest.

Optimal placement of the membrane. Four different membrane locations, shown in Fig. 3a, are compared for maximal noise cancellation in the ear. Location #1 is on the anterior notch of the pinna, location #2 is on the tragus, location #3 is in the cavum concha, and location #4 is on the lobule. The test results performed on the left synthetic ear of the HATS are shown in Fig. 3b, where the primary source signal is a broadband grey noise with a customised Fletcher-Munson curve filter⁴⁸ from 500 Hz – 6000 Hz (details in the Supplementary Fig. S1). The filter is applied here for the primary noise to obtain sound pressure level with flat frequency response inside the ear. The loudspeaker for generating the primary noise source is located 0.6 m away directly at the rear of the head. The overall sound pressure level (SPL) at the left tympanic membrane is 77.7 dB without ANC.

With ANC on, the performances at locations #1 and #2 are similar and the overall SPL being 69.2 dB and 70.9 dB, respectively; however, the noise reduction is only significant at frequencies of less than 4000 Hz. The sound propagating into the ear canal is similar to that around the anterior notch of the pinna in the high frequency range. Thus, the performance at location #1 is similar to that at location #2. The noise reduction at location #3 is the best with an overall SPL being 63.5 dB when ANC is on. The overall SPL is reduced by 14.2 dB in the whole frequency range from 500 Hz – 6000 Hz. Location #4, the lobule, is further away from the ear canal than any of the other selected locations. The effective frequency range of the noise reduction is only up to 3000 Hz with an about 6 dB increment from 5000 Hz – 6000 Hz. Based on the outcomes from this membrane location performance analysis, in the following experiments, location #3 (cavum concha) is chosen as the optimal location for the membrane.

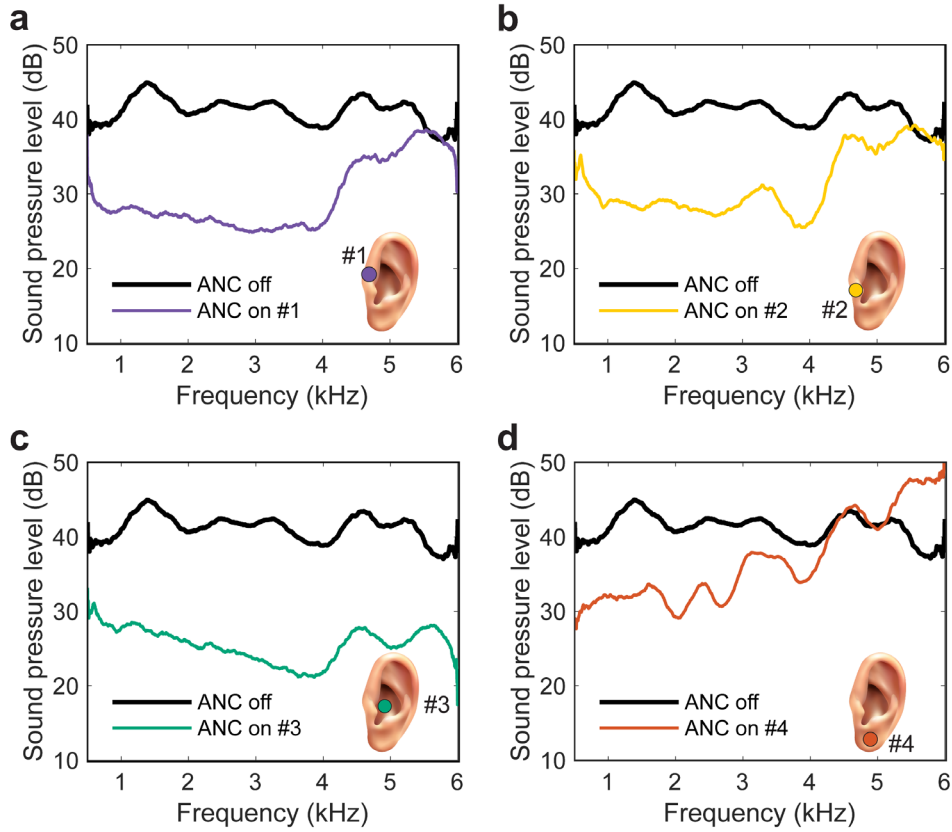


Figure 3. The sound pressure level at the left tympanic membrane measured from the HATS with and without the active noise cancellation (ANC), when (a) the membrane is at location #1, the *anterior notch*; (b) the membrane is at location #2, the *tragus*; (c) the membrane is at location #3, the *cavum concha*; and (d) the membrane is at location #4, the *lobule* of the left synthetic ear from the HATS.

Measurements for a stationary subject. Figure 4 shows the noise spectrum in two ears without and with ANC for three different primary sound fields. Here, multiple loudspeakers with identical signals are used to generate noise from different directions simultaneously. The primary source signal used is the same broadband grey noise used previously to obtain the results presented in Fig. 3. The measurement results are taken from the HATS, where the measured SPLs stand for the noise received at the tympanic membrane by a person. Figure 4a shows a scenario where a single primary loudspeaker is located 0.6 m away directly to the rear of the HATS to simulate the noise coming from a nearby place without considering any reflections from the surroundings in practice. Almost 15 dB attenuation are

obtained with the overall SPL changing from 78.1 dB to 63.8 dB at the left ear, and from 77.3 dB to 62.0 dB at the right ear. The scenario is similar to the one presented in the state-of-the-art system²⁵, where the noise with a bandwidth of up to 1000 Hz is controlled.

Figure 4b shows the results from a situation in which two primary loudspeakers are placed arbitrarily at two different locations. Approximately 13 dB attenuation is obtained with the overall SPLs changing from 80.2 dB and 77.9 dB to 66.0 dB and 65.2 dB at the left and right ears, respectively. This situation represents the situation with two original noise sources or a source near a large rigid surface, i.e. where one of the two primary speakers represents the reflection of the other noise source. Fig. 4c shows a more practical situation, where there are many primary noise sources to simulate the reflections coming from many directions. Four primary loudspeakers are placed arbitrarily at different locations to represent this situation. Approximately 11 dB attenuation is obtained with the overall SPL changing from 80.4 dB to 68.9 dB at the left ear and from 80.1 dB to 69.4 dB at the right ear. In all three of the selected scenarios, this system exhibits a minimum of 10 dB reduction in the entire ultra-broadband frequency range from 500 Hz – 6000 Hz.

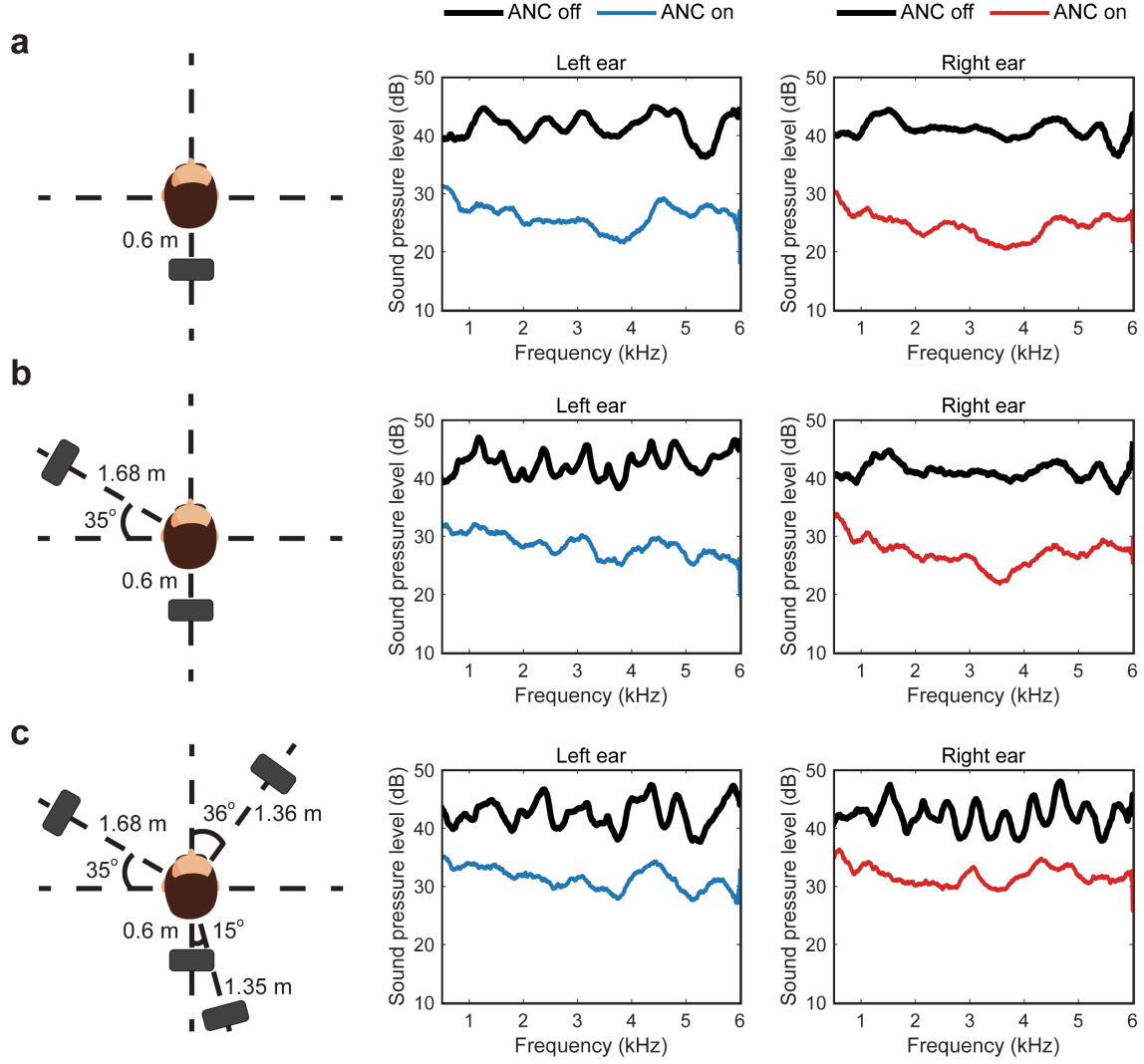


Figure 4. Three configurations of the primary loudspeakers and the corresponding sound pressure level (SPL) with and without active noise cancellation (ANC) at two ears. **(a)** A single primary loudspeaker is used to simulate the noise from a single noise source nearby. **(b)** Two primary loudspeakers are used to simulate two noise sources nearby or a single noise source with a nearby reflecting surface. **(c)** Four primary loudspeakers are used to simulate the noise coming from multiple directions, approximating a general case in practice.

Head tracking system. A human user is prone to move constantly, and the laser beam should therefore be able to track the corresponding movement of the membrane in the ears. A camera-based tracking

system is developed and implemented for the scenario described in Fig. 4a. The extended experimental setup, albeit for a single ear, is shown in Supplementary Fig. S2. The movement of the head (the movement of the membrane, to be exact) is tracked by a camera-based, bespoke image tracking system. Analogue voltage outputs, which are directly related to the position of the point-of-interest in two orthogonal directions (x and y), are connected to a motion controller with the pan and tilt galvanometer mirrors used to steer the laser beam to the required location. A circular yellow piece of tape is adhered on to the ear lobule as a marker for the object tracking purpose. After setting the laser beam to the centre of the membrane at the initial stage, the controller detects any relative movement between the membrane and the tracker in the process and adjusts the steering mirrors so that the laser beam remains on the membrane for the LDV to sense the sound pressure error signal required for the ANC in the same way as that for the stationary scenario described in the previous section.

The Supplementary Movie shows the results for both a stationary listener with ANC on and off and for a moving listener with tracking enabled and disabled when ANC is on. For a moving listener, the HATS is used again for consistent results with the stationary scenario. The movement of the HATS is controlled manually. The front-back movement is used to imitate a real person moving back and forth. Figure 5a shows the time domain measurement of these four situations, where each situation lasts for 15 seconds. Figure 5b shows the corresponding averaged frequency spectrum for each situation for the entire 15 second duration. As for the equivalent results previously presented in Fig. 4, the total SPL is reduced from 81.1 dB to 64.1 dB over the 500 Hz – 6000 Hz range for the stationary situation. When the HATS moves with ANC on but without tracking, the total SPL can increase significantly, and the system has the tendency of diverging.

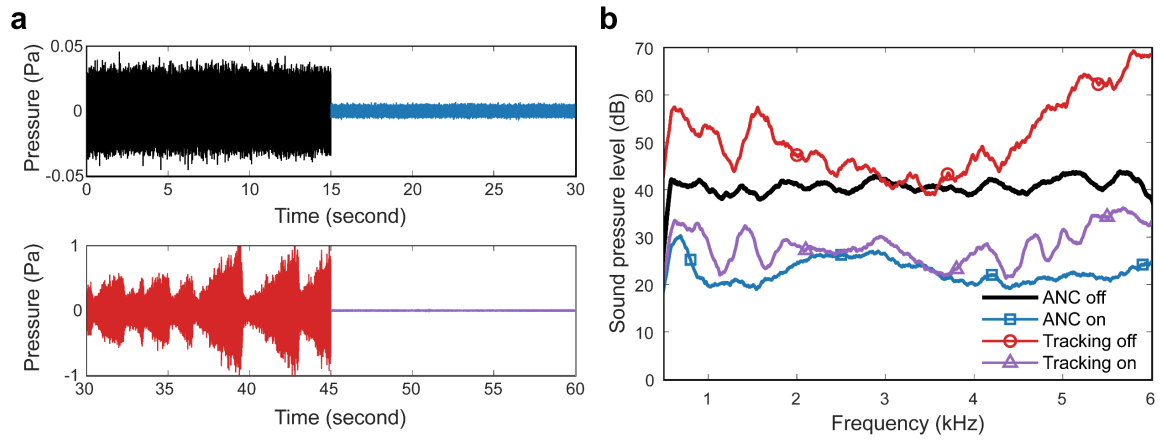


Figure 5. The ANC performance with the developed head tracking system. **(a)** The time domain signal at the tympanic membrane measured by the head and torso simulator (HATS) for 60 seconds. The top 30 seconds show the sound pressure with active noise cancellation (ANC) off and on for the stationary situation, the bottom 30 seconds show the sound pressure with ANC on when the tracking is turned off and on for a moving listener (each lasts for 15 seconds). **(b)** The corresponding spectrum of the signals, where the curve labelled with “ANC on” shows the spectrum of the residual noise for the stationary situation with ANC on, while the curves labelled with “Tracking off” and “Tracking on” show that for the moving situations after ANC without and with tracking.

Discussion

We propose a novel error sensing methodology for noise cancellation at a listener’s ears. For personal hearing protection, the proposed optical microphone arrangement shows many advantages. Unlike traditional methods which involve placing microphones at remote locations to estimate the noise at the ears, the laser beam from the LDV can be pointed to any desired location for measurements without contact and with a negligible footprint size. Thus, a “virtual ANC headphone” system with optical microphones can be realised to achieve non-intrusiveness for the listener while cancelling the noise. Since it can be directed very nearby to the ear canal entrance, the system can suppress noise over an ultra-broadband range, i.e. up to 6000 Hz as demonstrated herein. With a robust, camera vision-based

head tracking system incorporated, this system can tolerate user's movements while cancelling the noise.

This system can be readily adopted for headrests in airplanes or automotive applications and even within offices and households. It also has potential in medical applications, for example, protecting infants from medical equipment noise in the neonatal intensive care units⁴⁹ or for assisting people who suffer with broken sleep as a result of unwanted noise from snoring or other sources⁵⁰. In this latter case, only a minimal number of devices can be installed on the user during the sleep.

We acknowledge some of the limitations of the system presented in this paper. Firstly, although we used multiple primary sources to simulate the noise coming from random directions, the reference signal is taken directly from the primary loudspeakers, which is unknown in the real situation. Secondly, the head tracking system shown for illustration is only capable of tracking two-dimensional motions. A more robust head tracking system can be designed for three-dimensional movements. Lastly, it should be noted that the laser type used in the experiment is Class 2 Helium-Neon laser. Although it is eye-safe, it can cause undesirable glare to the user. Invisible infrared light can, however, be used for eyesight protection in future developments.

The proposed optical microphone can be used in many other applications where the use of a ordinary microphone is precluded. The demonstrated laser beam steering system can be used to allow the optical microphone to sequentially measure the sound at multiple locations rapidly. This is beneficial to the situation where interference may be caused from the presence of multiple microphones. Moreover, not only can the proposed virtual ANC headphone system be used for noise cancellation, but also it can be applied to sound reproduction and enhancement as well as spatial audio in virtual reality and augmented reality. A wide range of applications become available through the research and development of this system.

Methods

Noise cancellation algorithm. The ANC controller uses the feedforward configuration with the filtered-x LMS (FxLMS) algorithm^{51,52}, which is one of the most robust adaptive algorithms in active control. The general block diagram is shown in Fig. 1c and the detailed block diagram of the algorithm are shown in the Supplementary Fig. S3. At each side of the ear, the reference signal $x(n)$ is taken from the primary source for the adaptive ANC controller to calculate the control signal $y(n)$ for the secondary loudspeaker. (Subscripts L and R for “Left” and “Right” are omitted for clarity.) An LDV measures the error signal $e(n)$, which can be represented as

$$e(n) = p(n) + \mathbf{w}^T \hat{\mathbf{r}}(n) \quad (3)$$

where \mathbf{w} is the vector of controller coefficients and $\hat{\mathbf{r}}(n)$ is the estimated filtered reference signal vector from the impulse response of the estimated secondary path filter $\hat{s}(n)$, which is calculated by

$$\hat{\mathbf{r}}(n) = \hat{s}(n) * \mathbf{x}(n) \quad (4)$$

where $\mathbf{x}(n)$ is the reference signal vector. The controller coefficients are updated with

$$\mathbf{w}(n+1) = \mathbf{w}(n) - \mu \hat{\mathbf{r}}(n) e(n) \quad (5)$$

where μ is the convergence coefficient. The error signal $e(n)$ is the vibration velocity from the LDV in this case.

Experimental apparatus. The HATS used as a stationary subject is from Brüel and Kjær (Type 4128-C). The right and left ear simulators are embedded inside the heads to measure the sound received at the tympanic membranes in a human. The LDV used for measuring the residual sound is a Polytec PDV-100 Portable Digital Vibrometers. It has a compact size and an excellent precision of $< 20 \text{ nm/s}/\sqrt{\text{Hz}}$ with the measurable frequency range from 0.5 Hz to 22000 Hz. Two LDVs (one for each ear) are mounted on a tripod, which is isolated from the HATS or loudspeakers to avoid interference. The ANC

controller used for adaptive control is an Antysound TigerANC WIFI-Q controller. In the configuration of the controller, the sampling rate is 32000 Hz, and the lengths for both primary and secondary paths are set to 1024. All loudspeakers used are Genelec 8010A.

Membrane design. The membrane used in the experiment is a high-gain retro-reflective tape with pre-coated adhesive. Like a condenser microphone, the retro-reflective tape works similarly as a microphone diaphragm, and the substrate is similar to the microphone cartridge. However, unlike a microphone, there is neither any electronic components inside to process the measured signal, nor the need of wiring for the signal. The data acquisition system is in the LDV in this optical microphone arrangement. Due to the need to place the membrane in listener's ears, the dimension of the structure is limited. The structure used in this demonstration has a diameter of 9.2 mm and a height of 4.6 mm, with a weight of approximately 0.2 g. The membrane has good mechanical response to the sound with a small diameter that can be fitted into one's ear.

Tracking system. The LDV used with the tracking system is a Polytec NLV-2500-S laser vibrometer, which is placed 0.3 m away from the left ear of the HATS. The measurement sensitivity is set to 5 mm/s/V leading to a typical resolution of 20 nm/s/ $\sqrt{\text{Hz}}$. The controller used in the demonstration for the object tracking is the Raspberry Pi 3B+, accompanied with a 5MP Omnivision 5647 camera module for Raspberry Pi at 30 fps. MCP4725 Digital-to-Analogue Converter is used to convert the digital signals from the Raspberry Pi to analogue signals for the galvanometer mirrors. The galvanometer mirrors are from GSI Lumonics with a matching driver MiniSAX.

The recognition of the object is implemented through the colour extraction in OpenCV. A yellow marker (shown in Supplementary Fig. S2) is chosen in the demonstration. The marker is extracted using an adequate threshold of a series of colour images. The image becomes binary as

$$B(x, y) = \begin{cases} 0 & (\text{elsewhere}) \\ 1 & (I(x, y) > T) \end{cases} \quad (6)$$

where $I(x,y)$ and $B(x,y)$ are the pixel value of the original image and the binarised image, respectively. T is the threshold for the chosen marker.

Due to the circular shape of the marker, the centre of mass of the target object can be easily calculated, which is the centre of the marker. Between each two frames, the pixel shift of this centre is used to obtain the moving velocity of the object $\mathbf{v}_p(x,y)$. It can translate to the moving velocity of the target object in reality $\mathbf{v}_r(x,y)$, which is expressed as

$$\mathbf{v}_r(x,y)\Big|_D = S\mathbf{v}_p(x,y) \quad (7)$$

where S is a scaling factor for a given distance D between the camera and the target object. The value of S can be found during the calibration stage.

Data availability

The data that support the findings of this study are available from the authors on reasonable request, see author contributions for specific data sets.

References

1. Zhou, X. & Merzenich, M. M. Environmental noise exposure degrades normal listening processes. *Nat. Commun.* **3**, (2012).
2. Stansfeld, S. A. & Matheson, M. P. Noise pollution: Non-auditory effects on health. *Br. Med. Bull.* **68**, 243–257 (2003).
3. Stansfeld, S. *et al.* Aircraft and road traffic noise and children's cognition and health: a cross-national study. *Lancet* **365**, 1942–1949 (2005).
4. Elliott, S. J. *Signal processing for active control*. (Academic Press, 2000).
5. Berger, E. H. & Casali, J. G. Hearing Protection Devices. in *Encyclopedia of Acoustics* 967–981 (John Wiley & Sons, Inc., 2007).
6. Arenas, J. P. & Crockert, M. J. Recent Trends in Porous Sound-Absorbing Materials. *J. Sound Vib.* 12–17 (2009).
7. Bai, M. R., Pan, W. & Chen, H. Active feedforward noise control and signal tracking of headsets: Electroacoustic analysis and system implementation. *J. Acoust. Soc. Am.* **143**, 1613–1622 (2018).
8. Zhang, L. & Qiu, X. Causality study on a feedforward active noise control headset with different noise coming directions in free field. *Appl. Acoust.* **80**, 36–44 (2014).
9. Zevitas, C. D. *et al.* Assessment of noise in the airplane cabin environment. *J. Expo. Sci. Environ. Epidemiol.* **28**, 568–578 (2018).
10. Feist, J. P., Mongeau, L. & Bernhard, R. J. Tollbooth Operators' Response to Traffic Noise and the Performance of an Active Noise Control Headset: Survey Results. *Transp. Res. Rec. J. Transp. Res. Board* **1756**, 68–75 (2001).

11. Babisch, W., Beule, B., Schust, M., Kersten, N. & Ising, H. Traffic noise and risk of myocardial infarction. *Epidemiology* **16**, 33–40 (2005).
12. Selander, J. *et al.* Long-Term Exposure to Road Traffic Noise and Myocardial Infarction. *Epidemiology* **20**, 272–279
13. Evans, G. W. & Johnson, D. Stress and open-office noise. *J. Appl. Psychol.* **85**, 779–783 (2000).
14. Olson, H. F. & May, E. G. Electronic Sound Absorber. *J. Acoust. Soc. Am.* **25**, 1130–1136 (1953).
15. Garcia-Bonito, J., Elliott, S. J. & Boucher, C. C. Generation of zones of quiet using a virtual microphone arrangement. *J. Acoust. Soc. Am.* **101**, 3498–3516 (1997).
16. Rafaely, B., Elliott, S. J. & Garcia-Bonito, J. Broadband performance of an active headrest. *J. Acoust. Soc. Am.* **106**, 787–793 (1999).
17. Elliott, S. J. & Jones, M. An active headrest for personal audio. *J. Acoust. Soc. Am.* **119**, 2702–2709 (2006).
18. Buck, J., Jukkert, S. & Sachau, D. Performance evaluation of an active headrest considering non-stationary broadband disturbances and head movement. *J. Acoust. Soc. Am.* **143**, 2571–2579 (2018).
19. Jung, W., Elliott, S. J. & Cheer, J. Local active control of road noise inside a vehicle. *Mech. Syst. Signal Process.* **121**, 144–157 (2019).
20. Elliott, S. J. & David, A. A virtual microphone arrangement for local active sound control. in *Proc. 1st International Conference on Motion and Vibration Control* 1027–1031 (The Society, 1992).
21. Roure, A. & Albarrazin, A. The remote microphone technique for active noise control. in

- INTER-NOISE and NOISE-CON Congress and Conference Proceedings* **1999**, 1233–1244 (1999).
22. Cazzolato, B. S. Sensing Systems for Active Control of Sound Transmission into Cavities. *Mech. Eng.* (1999).
 23. Moreau, D., Cazzolato, B., Zander, A. & Petersen, C. A review of virtual sensing algorithms for active noise control. *Algorithms* **1**, 69–99 (2008).
 24. Jung, W., Elliott, S. J. & Cheer, J. Estimation of the pressure at a listener’s ears in an active headrest system using the remote microphone technique. *J. Acoust. Soc. Am.* **143**, 2858–2869 (2018).
 25. Elliott, S. J., Jung, W. & Cheer, J. Head tracking extends local active control of broadband sound to higher frequencies. *Sci. Rep.* **8**, (2018).
 26. Jung, W., Elliott, S. J. & Cheer, J. Combining the remote microphone technique with head-tracking for local active sound control. *J. Acoust. Soc. Am.* **142**, 298–307 (2017).
 27. Cummer, S. A., Christensen, J. & Alù, A. Controlling sound with acoustic metamaterials. *Nat. Rev. Mater.* **1**, 16001 (2016).
 28. Assouar, B. *et al.* Acoustic metasurfaces. *Nature Reviews Materials* **3**, 460–472 (2018).
 29. Liu, Z. *et al.* Locally resonant sonic materials. *Science* **289**, 1734–6 (2000).
 30. Christensen, J., Martín-Moreno, L. & García-Vidal, F. J. All-angle blockage of sound by an acoustic double-fishnet metamaterial. *Appl. Phys. Lett.* **97**, (2010).
 31. Xie, Y. *et al.* Wavefront modulation and subwavelength diffractive acoustics with an acoustic metasurface. *Nat. Commun.* **5**, (2014).

32. Liang, B., Guo, X. S., Tu, J., Zhang, D. & Cheng, J. C. An acoustic rectifier. *Nat. Mater.* **9**, (2010).
33. Popa, B. I. & Cummer, S. A. Non-reciprocal and highly nonlinear active acoustic metamaterials. *Nat. Commun.* **5**, 3398 (2014).
34. Popa, B. I., Zhai, Y. & Kwon, H. S. Broadband sound barriers with bianisotropic metasurfaces. *Nat. Commun.* **9**, 1–7 (2018).
35. Khanikaev, A. B., Fleury, R., Mousavi, S. H. & Alù, A. Topologically robust sound propagation in an angular-momentum-biased graphene-like resonator lattice. *Nat. Commun.* **6**, (2015).
36. Bilaniuk, N. Optical microphone transduction techniques. *Appl. Acoust.* **50**, 35–63 (1997).
37. Rothberg, S. J. *et al.* An international review of laser Doppler vibrometry: Making light work of vibration measurement. *Opt. Lasers Eng.* **99**, 11–22 (2017).
38. Goode, R. L., Ball, G., Nishihara, S. & Nakamura, K. Laser Doppler vibrometer (LDV)--a new clinical tool for the otologist. *Am. J. Otol.* **17**, 813–22 (1996).
39. Rosowski, J. J., Mehta, R. P. & Merchant, S. N. Diagnostic utility of laser-Doppler vibrometry in conductive hearing loss with normal tympanic membrane. *Otol. Neurotol.* **24**, 165–75 (2003).
40. Ball, G. R., Huber, A. & Goode, R. L. Scanning laser Doppler vibrometry of the middle ear ossicles. *Ear. Nose. Throat J.* **76**, 213–8, 220, 222 (1997).
41. Davis, Q. V. & Kulczyk, W. K. Vibrations of turbine blades measured by means of a laser. *Nature* **222**, 475–476 (1969).
42. Chen, L., Zhang, D., Zhou, Y., Liu, C. & Che, S. Design of a high-precision and non-contact dynamic angular displacement measurement with dual-Laser Doppler Vibrometers. *Sci. Rep.* **8**, 1–11 (2018).

43. Halkon, B. J. & Rothberg, S. J. Vibration measurements using continuous scanning laser vibrometry: Advanced aspects in rotor applications. *Mech. Syst. Signal Process.* **20**, 1286–1299 (2006).
44. Nelson, P. A. & Elliott, S. J. *Active control of sound*. (Academic Press, 1991).
45. Zuckerwar, A. J. Theoretical response of condenser microphones. *J. Acoust. Soc. Am.* **64**, 1278–1285 (1978).
46. Homentcovschi, D. & Miles, R. N. An analytical-numerical method for determining the mechanical response of a condenser microphone. *J. Acoust. Soc. Am.* **130**, 3698–3705 (2011).
47. Lavergne, T., Durand, S., Bruneau, M., Joly, N. & Rodrigues, D. Dynamic behavior of the circular membrane of an electrostatic microphone: Effect of holes in the backing electrode. *J. Acoust. Soc. Am.* **128**, 3459–3477 (2010).
48. Fletcher, H. & Munson, W. A. Loudness, Its Definition, Measurement and Calculation. *Bell Syst. Tech. J.* **12**, 377–430 (1933).
49. Zimmerman, E. & Lahav, A. Ototoxicity in preterm infants: Effects of genetics, aminoglycosides, and loud environmental noise. *J. Perinatol.* **33**, 3–8 (2013).
50. Ulfberg, J., Carter, N., Talbäck, M. & Edling, C. Adverse health effects among women living with heavy snorers. *Health Care Women Int.* **21**, 81–90 (2000).
51. Kuo, S. M. & Morgan, D. R. *Active noise control systems: algorithms and DSP implementations*. (Wiley, 1996).
52. Hansen, C., Snyder, S., Qiu, X., Brooks, L. & Moreau, D. *Active Control of Noise and Vibration*. (CRC Press, 2012).

Acknowledgements

We thank Shuping Wang, Qiaoxi Zhu, Sipei Zhao, Somanath Pradhan and Jiaxin Zhong's help during the development of the experiments. We thank Mr. Chris Chapman for constructing the scanning system. Special thanks to Sipei Zhao for providing helpful discussions and Sebastian Oberst for reviewing the manuscript.

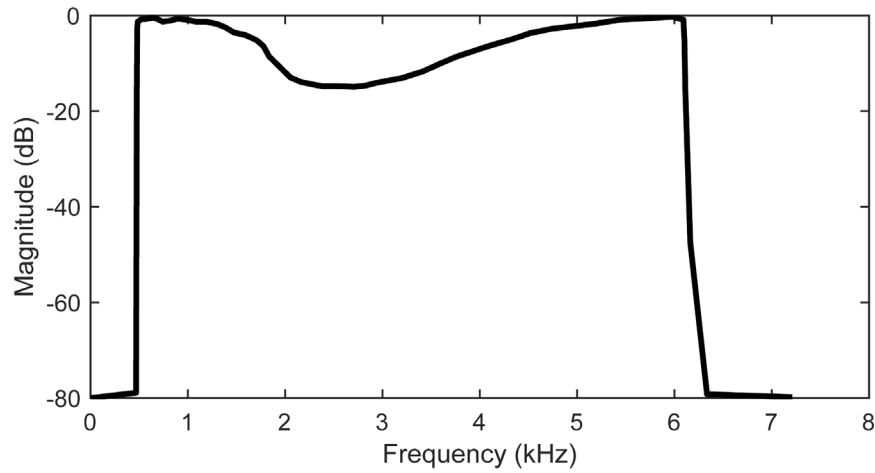
Author Contributions

T.X. contributed to idea conception, experimental design and measurements, data analysis and writing of the manuscript. X.Q. initiated and supervised the study, contributed to idea conception and data analysis. B.H. advised on fundamentals of LDV and identified the need for the finite, scattering element – the membrane. All authors discussed and reviewed the manuscript.

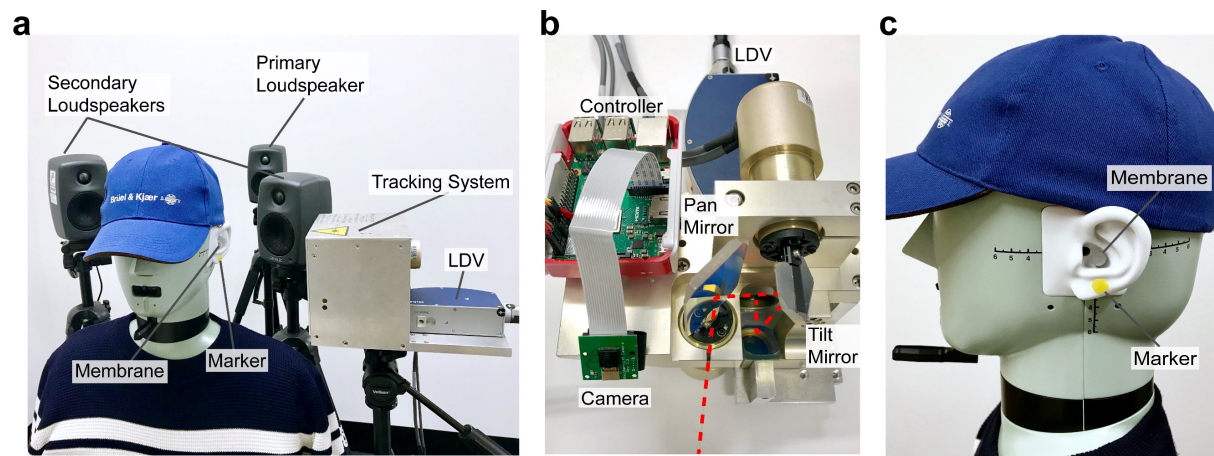
Additional Information

Competing interests: The authors declare no competing interests.

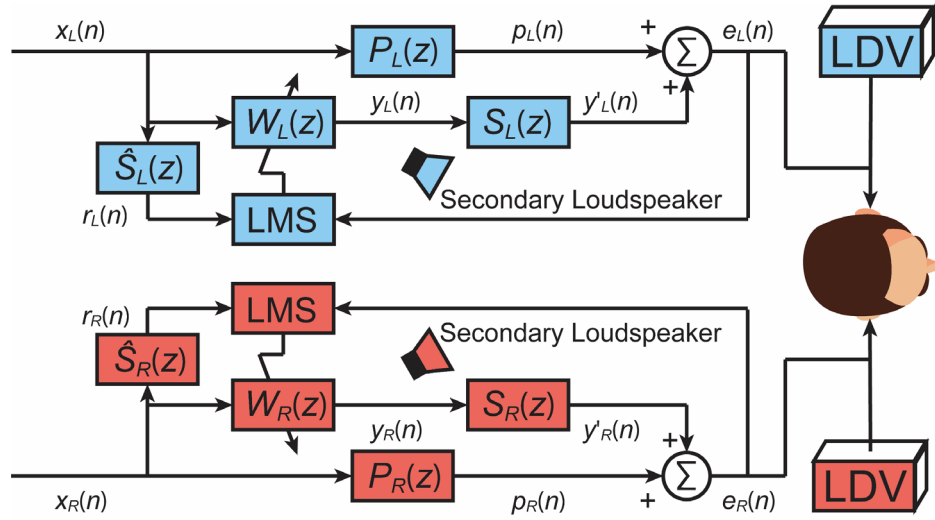
Supplementary information



Supplementary Figure S1. The spectrum of a customised Fletcher-Munson curve filter



Supplementary Figure S2. (a) Configuration of the head tracking system with a single primary loudspeaker. The tracking system and the laser Doppler vibrometer (LDV) are placed at the left side of the head. (b) The construction of the tracking system with a pan and a tilt mirror for steering the laser beam. The camera is attached to the controller for the target object tracking. (c) A yellow marker is placed below the membrane on the ear lobule as the target object.



Supplementary Figure S3. The block diagram of the adaptive active control algorithm for cancelling the vibration velocity of the membrane measured by an LDV at each ear.

Supplementary Movie – The virtual ANC headphone with head tracking